
Life Sequence Transformer: Generative Modelling for Counterfactual Simulation

Alberto Cabezas

Department of Economics and Statistics
University of Turin
alberto.cabezasgonzalez@unito.it

Carlotta Montorsi

Department of Economics and Statistics
University of Turin
carlotta.montorsi@unito.it

Abstract

Social sciences rely on counterfactual analysis using surveys and administrative data, generally depending on strong assumptions or the existence of suitable control groups, to evaluate policy interventions and estimate causal effects. We propose a novel approach that leverages the Transformer architecture to simulate counterfactual life trajectories from large-scale administrative records. Our contributions are: the design of a novel encoding method that transforms longitudinal administrative data to sequences and the proposal of a generative model tailored to life sequences with overlapping events across life domains. We test our method using data from the Istituto Nazionale di Previdenza Sociale (INPS), showing that it enables the realistic and coherent generation of life trajectories. This framework offers a scalable alternative to classical counterfactual identification strategy—such as difference-in-differences and synthetic controls—particularly in contexts where these methods are infeasible or their assumptions unverifiable. We validate the model’s utility by comparing generated life trajectories against established findings from causal studies, demonstrating its potential to enrich labour market research and policy evaluation through individual-level simulations.

1 Introduction

Counterfactual inference is a cornerstone of scientific reasoning in disciplines such as political science Sekhon [2009], economics [Heckman, 2008], history [Levy, 2015], and psychology [Foster, 2010], and has also sparked ongoing methodological debate [Cartwright, 2007a]. Counterfactual identification requires constructing hypothetical scenarios that resemble what would have happened in the absence of an event assumed to be causal [Rubin, 2005]. Such a scenario allows quantifying the impacts of specific events—like treatments or policies—or the underlying causes of observed outcomes. Typical research questions include: What is the causal effect of increasing the minimum wage on household consumption [Alonso, 2022]? What are the drivers of civil conflict [Acemoglu et al., 2020]?

The gold standard approach for identifying causal effects involves randomised interventions, in which the treatment is assigned randomly to some individuals and withheld from others [Cartwright, 2007b]. The difference in outcomes between the treated and control groups is interpreted as the causal effect of treatment. Randomisation ensures that characteristics that might correlate with the outcome of interest, such as gender, age, and socioeconomic status, are, on average, evenly distributed across the treatment and control groups. Thus, any systematic outcome difference can be attributed to the treatment itself.

However, randomisation rarely occurs naturally and can be challenging to implement even in controlled settings, due to ethical constraints and substantial costs [Thomas, 2016]. As a result, economists and other researchers have developed strategies and mathematical models to identify suitable control groups without relying on random treatment assignment. Despite being widely

adopted, these observational methods often rely on specific assumptions about the data and the underlying causal mechanisms, which are typically difficult to verify in practice (for instance, see Appendix A).

Our contributions This paper addresses a fundamental challenge in counterfactual inference: how to construct hypothetical scenarios that are both realistic and practically obtainable, especially when randomisation is unfeasible. We introduce a novel encoding method for life trajectories derived from administrative data in Section 3. Then, detail a Transformer foundational model for the generative task in Section 4. The model is trained on 1.6 million individual labour trajectories from INPS data, enabling scalable simulation of counterfactual life paths. In Section 5, our empirical analysis shows the generative potential of our encoding and architecture through two benchmarking exercises: evaluating its ability to simulate realistic life sequences aligned with traditional causal inference-driven findings in Section 5.2 and evaluating the coherence of generated out-of-sample trajectories in Section 5.3. Once trained, the model can generate realistic alternative life sequences by injecting or removing specific events from an individual’s observed trajectory, thus constructing counterfactuals without relying on external control groups.

2 Background

Our work builds on recent advances in Transformer-based sequence modelling for longitudinal labour and health data. In particular, Life2Vec [Savcisen et al., 2024], CAREER [Vafa et al., 2024], and TransformEHR [Yang et al., 2023]. Life2Vec showed the validity of encoder-only Transformer models for modelling socio-economic data and outperformed the predictive performance of standard models—like mortality tables, logistic regression, or recurrent neural networks—on individual’s future life outcomes (e.g., mortality) or time-invariant characteristics (e.g., personality nuances). However, their model lacks generative capability to simulate sequences of future tokens, and their data encoding cannot be easily adapted to a generative task. In contrast, our proposed encoding approach enables the training of a generative decoder, allowing for the simulation of counterfactual life sequences on a model architecture directly inspired by Life2Vec.

The CAREER encoder-decoder Transformer model focused on job sequence generation with annual temporal resolution and no rich occupational attributes, such as work province or work title. We enhance this framework by introducing fine-grained temporal encoding and a richer set of characteristics that span labour and demographic dimensions. In CAREER, time is introduced with a timestep of one year, and there is no way of modelling the duration of events or the exact timing of occurrence. You could increase the timestep to monthly steps, but this would restrict generation to a fixed monthly grid, offering no control over when within the year events begin or how long they last. Our method of encoding time, by contrast, enables flexible temporal generation by allowing each life event to have a defined starting month and duration in months within the year.

TransformEHR is an encoder-decoder Transformer generative model which encodes sequences of electronic health records and predicts the subsequent closest diagnoses (ICD-10 code). It includes demographic and time embeddings to model the numerical format of the visit date. TransformEHR was pre-trained to predict a patient’s future visits, complete ICD codes, given longitudinal ICD codes up to the current visit. Similarly to Life2Vec, the timing of each visit must be specified at inference time—meaning the model cannot decide when events occur, but only generate diagnoses for predefined dates. In contrast, our model allows the generation process to determine when events occur and the duration of each event. Crucially, our model supports variable event durations, which is essential for modelling life sequences that extend beyond instantaneous diagnoses.

Another relevant work is the REMI data encoding [Huang and Yang, 2020] within the Figaro encoder-decoder Transformer [von Rütte et al., 2023], which models sequences in the musical domain through structurally rich encodings. The encoding approach informs our design of temporally structured representations, which we adapt to model life events rather than notes. REMI encodes rhythmic structure using the beat-bar-phrase hierarchical structure in music into the sequence. Specifically, encoding a <Bar> event to indicate the beginning of a bar and the <Pos> events to point to certain locations within a bar. We use these representations in our encoding to represent the years and months when a given event occurs.

Finally, recent work on causal representation learning (e.g., Vafa et al. 2025, Gloeckle et al. 2024) explores debiased fine-tuning and interpretable interventions; however, it does not explore generative, individual-level counterfactuals. Our approach fills this gap by combining causal reasoning with sequence generation, enabling more nuanced and personalised estimations of treatment effects.

3 Data Encoding

We build on the work of Savcisens et al. [2024], where life events are concatenated into a sequence, with absolute and relative temporal information embedded as auxiliary attributes rather than forming the structural backbone of the sequence. Our encoding method imposes an explicit calendar-like structure on each life trajectory to support the sequential generation of future tokens. The entire observed work history is divided into yearly segments, each further subdivided into twelve monthly intervals, which are then populated with event information as needed. This structure mirrors the design used in music generation models [Huang and Yang, 2020]: yearly segments correspond to musical bars, and monthly divisions set the tempo within each bar. Each life event acts like a musical note, characterised by attributes such as employment type, work intensity, sector, and qualification, much like musical notes vary in pitch, duration, and intensity.

For instance, if an individual remains employed at the same firm for 10 uninterrupted years, we encode this as 10 events—each representing one full year with a 12-month duration—and each is described using the same set of tokens. In musical terms, this resembles a sustained note repeated across multiple bars. Conversely, if a person holds a one-year contract but experiences a one-month interruption, the year is split into two separate events with different durations, but otherwise described by the same set of concept-tokens. When no life event occurs within a year, the structure still records an "empty" year, analogous to a silent bar in a piece of music, preserving the regular temporal rhythm of the sequence. Figure 1 illustrates the encoding pipeline. We consider each tabular record (i.e., each row in the administrative dataset) as an *event or note* and translate each column describing it into a *concept-token*. Then, we concatenate all the events for a given individual in chronological order and create an individual sequence.

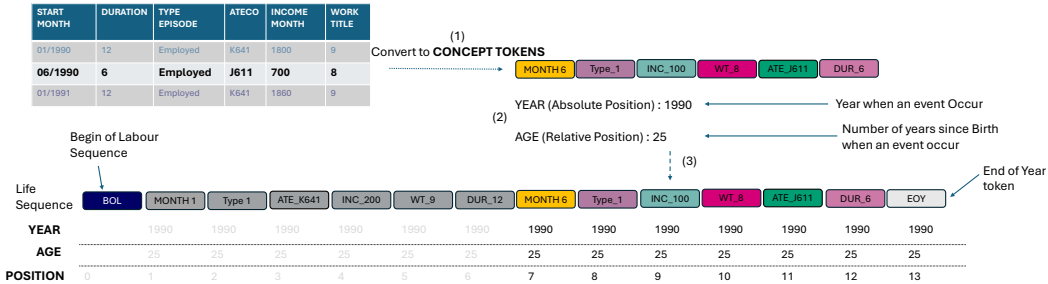


Figure 1: The step for converting data from Tabular format to the Generative model suitable format: (1) Convert relevant features to concept tokens (2) Look up relevant temporal information such as age and year (3) Concatenate token, time, and positional embeddings to the sequence.

Each event includes embeddings regarding positional information: year or *absolute* position reporting the calendar year when the event occurred, age or *relative* position with the individual’s age at the time of the event, and the usual *positional* embedding used in Transformer models for the position of the token in the sequence. These embeddings represent an absolute timeline (calendar year), a relative perspective (age at the time of event), and the position of the token within the sequence itself. These three embeddings are not part of the generative task, instead, they are deterministic.

Sequences start with the special token <BOL> (Beginning of Life). Individual events are then encoded using a fixed token order. <MONTH_X> marks the calendar month the event begins and helps separate multiple events within the same year. Next comes <TYPE_X> to indicate the event type (e.g., employment, unemployment), optionally followed by modifiers like <ATECO_X> (for sector)

and `<WRK_TITLE_X>` (for job title), depending on the event. `<DUR_X>` defines the event’s duration in months and concludes the event. If more events follow in the same year, another `<MONTH_X>` appears; otherwise, the sequence ends with `<EOY>` (End of Year), or if no further events exist, the entire life sequence ends. Each sequence maintains a consistent ordering of these concept-tokens, ensuring a structured representation and facilitating the learning of this artificial language.

While the experiments in this paper focus on labour-related life sequences, we emphasise that the proposed encoding scheme applies to other life domains, such as health and education. In the health domain, for instance, life sequences could represent diagnoses event attributes, annotated with the month of diagnosis and the duration of treatment or hospitalisation. Although a monthly resolution may appear too coarse for modelling certain health events, this limitation is mitigated by including intensity tokens `<INTENSITY_X>`, which capture the extent of engagement within each event’s duration. For a detailed description of the data and a labour life sequence example, see Appendix B.

Time-invariant individual information—such as gender, place and date of birth—is also represented using concept-tokens (e.g., `<F>` or `<M>` for female and male). Background information can be placed at the beginning of the sequence—allowing the entire input to be modelled as a single stream of tokens—or process it separately through a separate encoding architecture. The latter design distinguishes between static demographic attributes and the temporal sequence of life events, which begins with the `<BOL>` token, and allows the temporal sequence to be more directly influenced by these central life attribute parameters.

4 Transformer Models for Life Sequences

This section describes the encoder–decoder Transformer architecture, illustrated in Figure 7. We are presenting an encoder–decoder and a decoder-only version of our model (see Figure 6) and will compare them in the experiments to highlight their respective advantages and limitations. The only architectural difference between them is that, in the decoder-only setup, the background information is appended to the input sequence rather than processed separately. Contrarily, in the encoder–decoder setup, time-invariant covariates are processed by the encoder and used by the decoder through cross-attention to generate life trajectories. Both models are trained autoregressively to predict the next event in the sequence, conditioned on both past events and background information.

4.1 Model Architecture

The **decoder** block follows a standard Transformer decoder design, consisting of three components: an embedding block, stacked Transformer-based decoder layers, and a task-specific output head. We make three key modifications to the standard architecture. First, we replace the conventional attention mechanism with Performer Attention [Choromanski et al., 2022], which reduces the number of trainable parameters and improves computational efficiency. Second, we incorporate Rotary Position Embeddings (RoPE) [Su et al., 2023], adapted to work with Performer Attention, to better capture temporal patterns in the sequence. Third, to stabilise training, we apply RMS Normalisation [Zhang and Sennrich, 2019] before the attention and feedforward layers. The decoder uses causal (or masked) self-attention, ensuring that each token can only attend to earlier positions in the sequence, and cross-attention allows it to attend to the output of the encoder—conditioning on background characteristics. During training, the model is optimised using a next-token prediction objective, learning to generate coherent event sequences conditioned on prior events and time-invariant variables.

The **encoder** block processes the time-invariant background information, which consists of only four concept-tokens. Given the short length of this input, we use standard full self-attention without approximation. Positional embeddings are omitted, as the tokens are unordered and independent. RMS Normalisation is applied before both the attention and feedforward layers. The encoder outputs a fixed-length representation that conditions the decoder via cross-attention, but we do not implement it on all decoders; in the other layers, only self-attention is used (like in Figure 6). We treat the number of layers with cross-attention as a tunable hyperparameter. Although background information is relevant, tuning showed that allocating parameters to more self-attention-only layers is a more efficient use of parameters.

Token embeddings The first transformation of the input sequence occurs in the embedding layer, where each token in the sequence S_r is mapped to a continuous vector representation using an embedding matrix $\mathcal{E}_{\mathcal{V}} : \mathcal{V} \rightarrow \mathbb{R}^d$. Each row of $\mathcal{E}_{\mathcal{V}}$ corresponds to a unique token from the vocabulary \mathcal{V} , and each column represents one of the d embedding hidden dimensions. Following Savcisens et al. [2024], we center the embeddings by removing the mean from each matrix row.

Time embeddings To encode temporal information—specifically, age and calendar year—we use the Time2Vec method [Kazemi et al., 2019], which allows the model to capture both linear and periodic aspects of time. This method uses trainable parameters ω and φ to define a flexible sinusoidal function. We construct two separate time embeddings: one for age, denoted by $\mathcal{T}_A : \mathcal{A} \rightarrow \mathbb{R}^d$, and one for year, $\mathcal{T}_Y : \mathcal{Y} \rightarrow \mathbb{R}^d$. These embeddings are computed as:

$$\mathcal{T}(x)[z] = \begin{cases} \tanh(w_z x + \varphi_z) & \text{if } z \in [0, d//4) \text{ for Age or } z \in [0, d//2) \text{ for Year} \\ \sin(w_z x + \varphi_z) & \text{if } z \in [d//4, d) \text{ for Age or } z \in [d//2, d) \text{ for Year} \end{cases} \quad (1)$$

Initial iterations of the model used standard Time2Vec encoding, i.e. a linear component with trigonometric functions. However, we noticed that it led to poor out-of-sample performance: the model quickly lost coherence and failed to maintain the grammar of the life sequence when extrapolating beyond the training period. We hypothesised that this issue stemmed from the unbounded linear trend in the Time2Vec representation of age and year. Also, trigonometric components appeared to be mimicking linear trends—particularly for the year variable, but also for age.

Hence, we adapt the original Time2Vec by varying the proportion of linear and periodic components for different temporal signals and bounding the linear component for better out-of-sample generalisation (see Section 5.3). For year embeddings, we allocate a larger share of the hidden dimensions to the linear component (\tanh) to better capture the short-range time frame, which spans only 25 years. For the Age embedding, which spans 70 years in our dataset, we expand periodicity (\sin) to reflect cyclical patterns (e.g., retirement or career phases) that recur across broader age bands.

Positional embeddings In addition to temporal embeddings, we incorporate standard positional encodings to capture the order of tokens within each sequence. Our approach is adapted to use with local and global heads of Performer attention [Su et al., 2023]: sinusoidal positional encodings combined with RoPE in the global attention heads. Both positional and time embeddings are added to the token embeddings through a ReZero gate [Bachlechner et al., 2021] before being passed to the attention layers.

4.2 Training Procedure

Our dataset consists of 1,652,877 individual life sequences. We divide them into training (70%), validation (15%), and test (15%) subsets. The models are trained for 15 to 20 epochs with early stopping. Each training batch contains 24 sequences, and gradients are accumulated over four steps before an optimiser step, resulting in an effective batch size of 96. This enables stable training without requiring large amounts of GPU memory.

Optimization We employ the AdamW optimiser [Loshchilov and Hutter, 2019], with no weight decay applied to bias terms, embedding weights, or normalisation layers. The learning rate is controlled by the One Cycle policy [Smith and Topin, 2019] with a warm-up phase covering 30% of the training steps. Gradient norms are clipped at a maximum value of 5 to prevent exploding gradients. To avoid overfitting, a dropout rate of 10% is applied to the attention, feedforward, and embedding layers. Dataloaders and projection matrices of Performer attention are reloaded every epoch to ensure robustness in sampling. We use mixed-precision with `bf16`, which we chose to reduce memory usage and improve training efficiency, considering that RMS Normalisation has been shown to improve numerical stability in lower-precision regimes [Zhang and Sennrich, 2019].

Hyperparameters tuning We sample hyperparameters using the Tree-Structured Parzen Estimator [Watanabe, 2023] and Optuna [Akiba et al., 2019]. Experiments showed that larger models—especially with deeper networks—performed better. Without normalisation, the model misused the embedding space, often requiring unusually large embedding dimensions to compensate. With RMS normalisation, this effect was mitigated, although the model benefited from longer warmup

phases compared to setups using only ReZero. Increasing depth proved more effective than scaling up feedforward or embedding dimensions, or the number of random features. For local attention, we set the window size to cover approximately three complete events, which empirically balanced context coverage and memory use. Ultimately, we selected hyperparameters that maximized model capacity while fitting within the 16GB of VRAM available on an RTX A4000 GPU: 10 decoder layers for decoder-only and 8 decoder layers for encoder-decoder, only 2 with cross-attention, with 8 attention heads, 6 local with window size of 36 and 2 global with projection of 256 random features; 1 encoder layer with 2 attention heads; embedding size of 240, and position-wise feed forward size of 960 on all layers. Both models have around 7.1 million tunable parameters.

5 Empirical Analysis

In this section, we present the next-token prediction task metrics and evaluate the model’s ability to forecast out-of-sample for years beyond the training period. We also evaluate performance through a series of causal inference benchmarking exercises by comparing the generated life sequences against well-established empirical findings from labour economics. All experiments were run on both model variants, i.e. the encoder-decoder and the decoder-only architectures, and on the test subset of our data. In the main text, we present the best results and provide a discussion of how the two models compare across tasks, highlighting the strengths and weaknesses of each approach. The remaining results are included in Appendix E.

5.1 Next-Token Prediction Metrics

We begin by presenting the model’s performance on the next-token prediction task over the test subset. This task measures the model’s ability to correctly generate the next element in a life sequence, conditioned on all previous tokens and the encoded background information. Training each model took approximately 9 hours per epoch for the training phase and 1.5 hours per epoch for validation, totalling 10.5 hours per epoch. Since we train models between 15 and 20 epochs, depending on convergence, the total training time ranges between 158 and 210 hours per model.

Table 1 reports a standard set of classification metrics computed across the entire sequence dimension and vocabulary, excluding padding tokens. Each row corresponds to a different amount of observed history provided as input. Specifically, we generate the continuation of a life sequence after observing either zero, one, five, or ten years of past events. The metrics include macro-averaged accuracy, precision, recall, and F1 score, each evaluated using top 1 predictions, i.e. only the highest probability considered to find the correct label. We also report the square root cross-entropy loss, i.e. perplexity, a widely used measure in language modelling.

Both model variants achieve similar results on these metrics, so we report only the encoder-decoder results for brevity. As expected, the more historical context the model receives, the better it can predict future tokens. This is consistent with the intuition that individuals often follow relatively stable life patterns, e.g. remain within certain industries over time. Access to a longer sequence of past events enables the model to learn person-specific trajectories and reduces uncertainty about what is likely to happen next.

	Accuracy	Precision	Recall	F1 Score	Perplexity
0 known years	0.6236	0.6874	0.6236	0.6445	0.725
1 known year	0.6763	0.7179	0.6763	0.6872	0.696
5 known years	0.6869	0.7251	0.6869	0.6967	0.675
10 known years	0.7023	0.7382	0.7023	0.7108	0.6489

Table 1: **Encoder-Decoder** test set metrics for next-token prediction, macro-averaged across the vocabulary, conditioning on 0, 5, 1 and 10 initial years of sequence.

5.2 Causal Benchmarks

We evaluate the model’s capacity for generating causal relationships by testing whether it reproduces well-established causal effects from the labour economics literature and national policy. All generation experiments are run on batches of 8 sequences. On a GPU, generating the next token takes

approximately 0.2 seconds per batch, while on a CPU it takes about 2 seconds. We design three empirical exercises (more details are provided in Appendix D):

The first exercise is inspired by the finding that birth month causally impacts retirement timing [Ardito et al., 2020]. The mechanism behind this is that institutional timing (e.g., school starting in September, job transitions peaking in January) causes individuals born earlier in the year to begin and end schooling later, delaying their entry into the labour market. This delay propagates throughout life and leads to a slightly later retirement, observable in the timing of pension claims. We assess whether the model replicates this subtle but well-documented shift in retirement age based on birth month.

Figure 2 compares real and simulated retirement ages across birth cohorts, distinguishing between individuals born in January and December. The model successfully captures the expected empirical pattern: individuals born in December tend to retire earlier than those born in January, reflecting institutional rules that influence retirement timing. While it slightly overestimates the average retirement age, these predictions remain well within the confidence intervals of the real data, indicating that the model aligns closely with observed outcomes.

Figure 8 shows that the decoder-only model overestimates the mean of retirement ages more, while still preserving the expected negative effect of birth cohort on retirement age. Its weaker predictive accuracy highlights a consistent pattern across exercises where background information plays a central role: the decoder-only model, which receives background variables only as part of the initial sequence, struggles with their long-term influence. The encoder-decoder model incorporates this information via cross-attention, allowing for more targeted attention to the time-invariant attributes of the individual, at the cost of allocating fewer parameters to self-attention within the sequence.

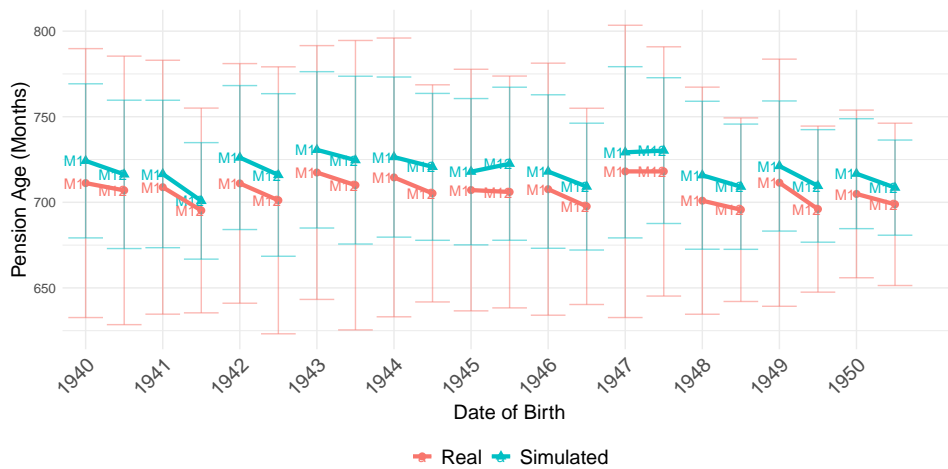


Figure 2: Real and **encoder-decoder** model-generated (blue) average pension ages—measured in months—for male individuals born between 1940 and 1950, stratified by birth month (January = M1, December = M12). Each point indicates the cohort-specific average retirement age for individuals born in January or December, with vertical bars representing a one standard deviation range.

The second exercise relates to the motherhood penalty, i.e. the long-term career setbacks women face after having children, often including reduced earnings and detachment from the labour market [Casarico and Lattanzio, 2023, Kleven et al., 2019]. We simulate mother’s careers from the moment of the first maternity leave event and compare the post-child trajectory with observed empirical trends.

Figure 3 compares the real and simulated income trajectories of mothers following their first childbirth. Synthetic sequences are generated conditionally on the sequence up to the maternity leave year. The model successfully captures the key features of the observed trends, closely replicating the average post-birth income dynamics. For this task, we report results from the decoder-only model, which demonstrates superior performance. We attribute this to the fact that background variables, like area of birth or age, play a limited role in explaining the after-birth trend, making the task particularly well-suited for models focused on local sequence patterns rather than long-range context. In contrast, Figure 9 shows how the encoder-decoder model’s predictive accuracy gradually declines the further we move away from the observed sequence.

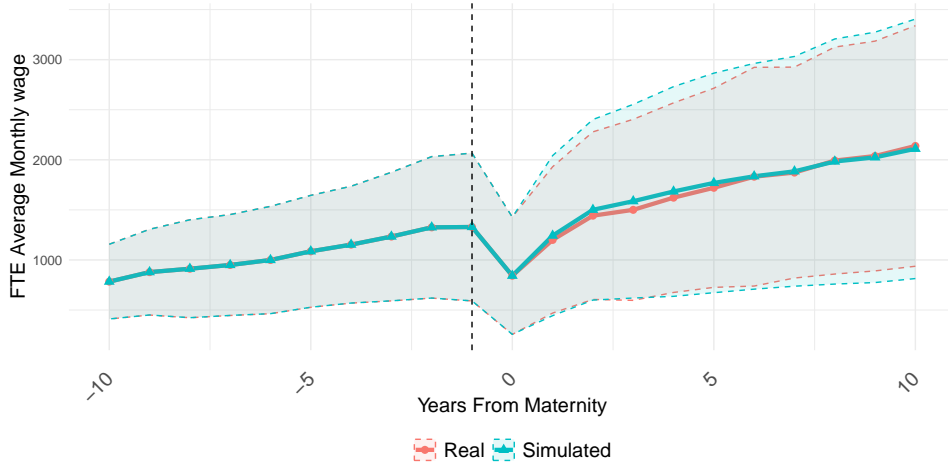


Figure 3: Real and **decoder-only** model-generated trajectories of average monthly income for working mothers in a 10-year window before and after their first maternity leave episode (Years From Maternity = 0). The solid lines represent the average monthly income, while the shaded areas denote the one standard deviation range.

Lastly, we evaluate the ability to generate the impact of an unemployment benefit policy rule in Italy. Until 2017, Italy’s mobility allowance granted income support to workers displaced due to firm closure. The benefit duration had discontinuities based on age (cutoff at 40 and 49) and region (South vs. North/Central), creating sharp jumps in benefit duration entitlement and reception [Brunello and Miniaci, 1997].

Figure 4 compares the real and simulated average duration of mobility allowance receipt. In the real data, we observe a statistically significant jump at the age 40 threshold, reflecting the policy rule. The simulated data captures the overall upward trend in benefit duration with age, suggesting that the model has learned the general relationship between age and benefit duration. However, it falls short of reproducing the sharp discontinuity observed at the age 40 threshold in the real data. While the simulated sequences reflect the correct direction of the trend, they smooth over the abrupt policy-induced change, indicating a limitation in the model’s sensitivity to this rule-based cutoff.

This underperformance is likely due to the low frequency of mobility allowance events in the training data, i.e. less than 1% of all sequences (see Figure 5), which limits the model’s ability to learn the underlying policy pattern. The decoder-only model, shown in Figure 12, fails to produce any significant change in benefit duration at the 40-year cutoff. This again highlights the limitations of the decoder-only approach in tasks where access to and emphasis on background variables, like age and region, are crucial for capturing policy-driven effects.

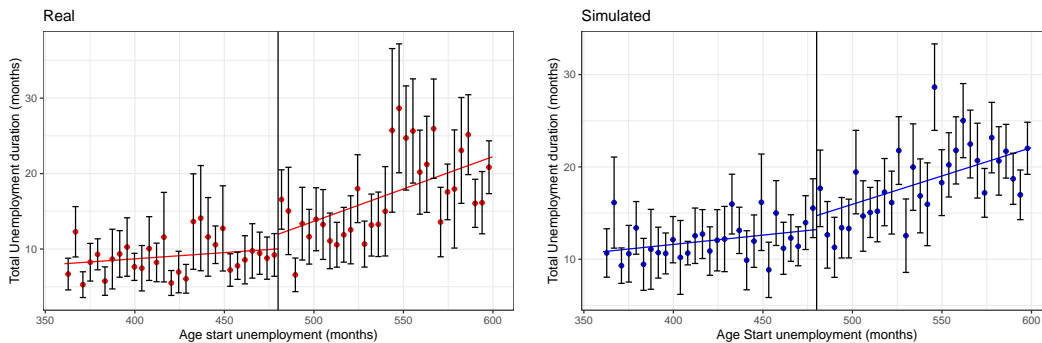


Figure 4: Real and **encoder-decoder** model simulated average duration with 90% confidence interval of mobility allowance receipt duration as a function of worker age at job loss in months in a 10-year bandwidth around the 40 years old threshold

5.3 Out-of-sample Generation

We evaluate the model’s out-of-sample performance by investigating the coherence of generated life sequences beyond the temporal window of the training data, i.e. after 2015. In this setting, the model is conditioned on observed sequences up to 2015 and generates tokens into the future. Though not explicitly necessary for counterfactual simulation, good out-of-sample performance indicates robustness, a desirable property for a model expected to simulate plausible scenarios.

Given the absence of ground truth data for these later years, our evaluation focuses on syntactic and structural correctness rather than predictive accuracy. Specifically, we examine the generated sequences for internal consistency, valid token ordering, and the absence of structural violations—such as overlapping events, misaligned episode boundaries, or implausible transitions. This assessment allows us to verify that the model preserves the learned "grammar" of life sequences when extrapolating beyond the observed data.

Figure 13 presents the density of years in which the first structural failure occurs for the decoder-only model, considering only sequences where a failure did occur within a 20-year generation window. The results show that most decoder-only sequences begin to fail around year 7 or 8, though a non-negligible share persists further, with successes becoming exponentially less likely as the generation horizon extends, and 5% of sequences remain structurally valid after 20 years. In contrast, the encoder–decoder model (Figure 14) exhibits earlier degradation, with most failures concentrated around year 4, very few sequences remaining valid beyond year 10 and none after year 20. These patterns confirm that decoder-only architectures are more robust for long-range generation tasks, maintaining structural coherence significantly longer than encoder–decoder counterparts.

6 Conclusion

We propose a novel encoding method for converting longitudinal administrative data into sequences and train two generative life sequence transformer models to simulate coherent and realistic counterfactual trajectories. The models are trained on a large-scale administrative dataset and optimised for next token prediction. Despite their relatively small size, the models show promising results in replicating well-known causal findings, showing the potential of lightweight architectures in this domain. We highlight the strengths of two architectural paradigms—decoder-only and encoder–decoder—across a range of causal generative tasks. In an out-of-sample sequence generation setting, the model remains functional, although token prediction accuracy and sequence coherence degrade increasingly with temporal distance from the training data.

Despite its promising performance, our model presents some limitations. As shown in the mobility allowance duration exercise, the model has less accurate generative capacities when used to generate sequences with events that are rare in the training data. This limitation is particularly relevant given the non-open nature of administrative data, which limits dataset sizes. This highlights the importance of fine-tuning the model for specific subpopulations or tasks. Additionally, the quality of sequence generation is sensitive to model architecture, introducing variability in counterfactual simulation tasks. Careful model selection and design are therefore essential; researchers must evaluate the trade-offs between architectures and systematically test and compare them to ensure robust results.

While the model offers a powerful tool for simulating policy scenarios and exploring counterfactual life trajectories, it raises important ethical and societal concerns. Predictive modelling of individual life courses—especially in domains such as employment, healthcare, or social services—carries the risk of reinforcing structural biases in the training data. There is also the potential for misuse, for example, in automated decision-making systems that influence resource allocation or eligibility for benefits, without appropriate human oversight or fairness safeguards. Out-of-sample generation into the future introduces further moral and philosophical concerns: guiding individuals’ lives based on generically generated futures could contribute to normative pressures or reductionist narratives. Our model’s limitations in long-range future prediction constrain such misuse, as it performs best when simulating counterfactuals within known historical periods. Nonetheless, any application of generative models to human trajectories must be governed by strict considerations of fairness, privacy, and security. Addressing these challenges will be critical to ensuring that such models are used responsibly, transparently, and in ways that support robust causal inference.

References

- A. Abadie, A. Diamond, and J. Hainmueller. Synthetic control methods for comparative case studies: Estimating the effect of california’s tobacco control program. *Journal of the American statistical Association*, 105(490):493–505, 2010.
- D. Acemoglu, L. Fergusson, and S. Johnson. Population and conflict. *The Review of Economic Studies*, 87(4):1565–1604, 2020.
- A. Agostinelli, T. I. Denk, Z. Borsos, J. Engel, M. Verzetti, A. Caillon, Q. Huang, A. Jansen, A. Roberts, M. Tagliasacchi, et al. Musiclm: Generating music from text. *arXiv preprint arXiv:2301.11325*, 2023.
- T. Akiba, S. Sano, T. Yanase, T. Ohta, and M. Koyama. Optuna: A next-generation hyperparameter optimization framework. In *Proceedings of the 25th ACM SIGKDD International Conference on Knowledge Discovery and Data Mining*, 2019.
- C. Alonso. Beyond labor market outcomes: The impact of the minimum wage on nondurable consumption. *Journal of Human Resources*, 57(5):1690–1714, 2022.
- C. Ardito, R. Leombruni, D. Blane, and A. d’Errico. To work or not to work? the effect of higher pension age on cardiovascular health. *Industrial Relations: A Journal of Economy and Society*, 59(3):399–434, 2020.
- T. Bachlechner, B. P. Majumder, H. Mao, G. Cottrell, and J. McAuley. Rezero is all you need: Fast convergence at large depth. In *Uncertainty in Artificial Intelligence*, pages 1352–1361. PMLR, 2021.
- A. Bena, R. Leombruni, M. Giraud, and G. Costa. A new italian surveillance system for occupational injuries: characteristics and initial results. *American journal of Industrial Medicine*, 55(7):584–592, 2012.
- G. Brunello and R. Miniaci. Benefit transfers in italy: an empirical study of mobility lists in the milan area. *Oxford Bulletin of Economics and statistics*, 59(3):329–347, 1997.
- D. Card and A. B. Krueger. Minimum wages and employment: A case study of the fast-food industry in new jersey and pennsylvania. *The American Economic Review*, 84(4):772–793, 1994. URL <http://www.jstor.org/stable/2118030>.
- F. Carta, A. Casarico, M. De Philippis, and S. Lattanzio. Mom’s out: employment after childbirth and firm-level responses. Technical report, IZA Discussion Papers, 2024.
- N. Cartwright. *Counterfactuals in Economics: A Commentary*, pages 191–216. Massachusetts Institute of Technology Press, 2007a.
- N. Cartwright. Are RCTs the gold standard? *BioSocieties*, 2(1):11–20, 2007b.
- A. Casarico and S. Lattanzio. Behind the child penalty: understanding what contributes to the labour market costs of motherhood. *Journal of Population Economics*, 36(3):1489–1511, 2023.
- K. Choromanski, V. Likhoshesterov, D. Dohan, X. Song, A. Gane, T. Sarlos, P. Hawkins, J. Davis, A. Mohiuddin, L. Kaiser, D. Belanger, L. Colwell, and A. Weller. Rethinking attention with performers, 2022. URL <https://arxiv.org/abs/2009.14794>.
- M. E. Consens, C. Dufault, M. Wainberg, D. Forster, M. Karimzadeh, H. Goodarzi, F. J. Theis, A. Moses, and B. Wang. Transformers and genome language models. *Nature Machine Intelligence*, pages 1–17, 2025.
- J. Devlin, M.-W. Chang, K. Lee, and K. Toutanova. Bert: Pre-training of deep bidirectional transformers for language understanding. In *Proceedings of the 2019 conference of the North American chapter of the association for computational linguistics: human language technologies, volume 1 (long and short papers)*, pages 4171–4186, 2019.
- E. M. Foster. Causal inference and developmental psychology. *Developmental Psychology*, 46(6): 1454, 2010.

- F. Gloeckle, B. Y. Idrissi, B. Rozière, D. Lopez-Paz, and G. Synnaeve. Better & faster large language models via multi-token prediction, 2024. URL <https://arxiv.org/abs/2404.19737>.
- J. J. Heckman. Econometric causality. *International statistical review*, 76(1):1–27, 2008.
- Y.-S. Huang and Y.-H. Yang. Pop music transformer: Beat-based modeling and generation of expressive pop piano compositions. In *Proceedings of the 28th ACM international conference on multimedia*, pages 1180–1188, 2020.
- L. S. Jacobson, R. J. LaLonde, and D. G. Sullivan. Earnings losses of displaced workers. *The American Economic Review*, pages 685–709, 1993.
- S. M. Kazemi, R. Goel, S. Eghbali, J. Ramanan, J. Sahota, S. Thakur, S. Wu, C. Smyth, P. Poupart, and M. Brubaker. Time2vec: Learning a vector representation of time, 2019. URL <https://arxiv.org/abs/1907.05321>.
- H. Kleven, C. Landais, and J. E. Sjøgaard. Children and gender inequality: Evidence from denmark. *American Economic Journal: Applied Economics*, 11(4):181–209, 2019.
- R. Leombruni, R. Quaranta, and C. Villosio. Note di pubblicazione di whip v. 3.2. *WHIP Technical Report No. 1/2010*, 2010.
- J. S. Levy. Counterfactuals, causal inference, and historical analysis. *Security Studies*, 24(3):378–402, 2015.
- I. Loshchilov and F. Hutter. Decoupled weight decay regularization, 2019. URL <https://arxiv.org/abs/1711.05101>.
- A. Radford, K. Narasimhan, T. Salimans, I. Sutskever, et al. Improving language understanding by generative pre-training. 2018.
- C. Raffel, N. Shazeer, A. Roberts, K. Lee, S. Narang, M. Matena, Y. Zhou, W. Li, and P. J. Liu. Exploring the limits of transfer learning with a unified text-to-text transformer. *Journal of Machine Learning Research*, 21(140):1–67, 2020.
- D. B. Rubin. Causal inference using potential outcomes: Design, modeling, decisions. *Journal of the American statistical Association*, 100(469):322–331, 2005.
- G. Savcisen, T. Eliassi-Rad, L. K. Hansen, L. H. Mortensen, L. Lilleholt, A. Rogers, I. Zettler, and S. Lehmann. Using sequences of life-events to predict human lives. *Nature Computational Science*, 4(1):43–56, 2024.
- J. S. Sekhon. Opiates for the matches: Matching methods for causal inference. *Annual Review of Political Science*, 12(1):487–508, 2009.
- L. N. Smith and N. Topin. Super-convergence: Very fast training of neural networks using large learning rates. In *Artificial intelligence and machine learning for multi-domain operations applications*, volume 11006, pages 369–386. SPIE, 2019.
- J. Su, Y. Lu, S. Pan, A. Murtadha, B. Wen, and Y. Liu. Roformer: Enhanced transformer with rotary position embedding, 2023. URL <https://arxiv.org/abs/2104.09864>.
- G. Thomas. After the gold rush: Questioning the “gold standard” and reappraising the status of experiment and randomized controlled trials in education. *Harvard Educational Review*, 86(3): 390–411, 2016.
- K. Vafa, E. Palikot, T. Du, A. Kanodia, S. Athey, and D. M. Blei. Career: A foundation model for labor sequence data, 2024. URL <https://arxiv.org/abs/2202.08370>.
- K. Vafa, S. Athey, and D. M. Blei. Estimating wage disparities using foundation models, 2025. URL <https://arxiv.org/abs/2409.09894>.
- A. Vaswani, N. Shazeer, N. Parmar, J. Uszkoreit, L. Jones, A. N. Gomez, Ł. Kaiser, and I. Polosukhin. Attention is all you need. *Advances in Neural Information Processing Systems*, 30, 2017.

- D. von Rütte, L. Biggio, Y. Kilcher, and T. Hofmann. Figaro: Controllable music generation using learned and expert features. In *The Eleventh International Conference on Learning Representations*, 2023.
- Y. Wang, H. Huang, C. Rudin, and Y. Shaposhnik. Understanding how dimension reduction tools work: An empirical approach to deciphering t-sne, umap, trimap, and pacmap for data visualization, 2021. URL <https://arxiv.org/abs/2012.04456>.
- S. Watanabe. Tree-structured parzen estimator: Understanding its algorithm components and their roles for better empirical performance, 2023. URL <https://arxiv.org/abs/2304.11127>.
- Z. Yang, A. Mitra, W. Liu, D. Berlowitz, and H. Yu. TransformEHR: transformer-based encoder-decoder generative model to enhance prediction of disease outcomes using electronic health records. *Nature Communications*, 14(1):7857, 2023.
- B. Zhang and R. Sennrich. Root mean square layer normalization. *Advances in Neural Information Processing Systems*, 32, 2019.

A Difference-in-differences

Difference-in-differences (DiD) is one of the more commonly used causal identification strategies to evaluate the effects of policy interventions by comparing changes in an outcome variable between a treatment group and a control group, both before and after the intervention. Here, the main assumption is that the treated and control groups would have followed parallel trends over time in the absence of the policy or event under evaluation. This assumption, while critical, is rarely validated and often debated in empirical applications.

Card and Krueger [1994] on minimum wage in New Jersey is considered one of the most famous DiD studies; the authors compared employment in the fast food sector in New Jersey and in Pennsylvania, in February 1992 and in November 1992, after New Jersey's minimum wage rose from \$4.25 to \$5.05 in April 1992. Observing a change in employment in New Jersey only, before and after the treatment, would fail to control for omitted variables such as weather and macroeconomic conditions of the region. By including Pennsylvania as a control in a difference-in-differences model, any bias caused by shared variables between New Jersey and Pennsylvania is implicitly controlled for, even when these variables are unobserved. Assuming that New Jersey and Pennsylvania have parallel trends over time, Pennsylvania's change in employment can be interpreted as the change New Jersey would have experienced had it not increased the minimum wage, and vice versa. The evidence suggested that the increased minimum wage did not induce a decrease in employment in New Jersey, contrary to what some economic theory would suggest.

A.1 Event Study

While powerful, DiD is not always applicable, especially in settings where no natural control group exists. Consider, for example, the question: What is the causal effect of childbirth on a woman's career trajectory? Ideally, one would randomise fertility to estimate this effect, but such an experiment is infeasible. Applying DiD would require identifying a group of women identical to mothers in both observable and unobservable characteristics, and then assuming their career paths would have evolved similarly, absent childbirth. In practice, achieving such a match is highly challenging.

In such cases, researchers often turn to an event study design [Jacobson et al., 1993], a generalisation of DiD that exploits variation in treatment timing. Event studies are especially useful when all units are eventually treated at different times. The method compares changes in outcomes before and after treatment for each unit, leveraging variation across units treated at different points in time. In the childbirth example, this allows for estimating treatment effects by aligning individuals around the "event" (birth of a child) and comparing pre- and post-treatment trajectories. Like DiD, event studies rely on a version of the parallel trends assumption—that, absent the event, the trajectory of the outcome would have continued as observed in the pre-treatment period.

A.2 Synthetic Control

The Synthetic Control Method (SCM) is another causal inference approach closely related to difference-in-differences. It is particularly well-suited to cases where a single unit (such as a country, region, or firm) undergoes treatment, and no comparable control group exists. Instead of relying on a parallel trends assumption between predefined groups, SCM constructs a synthetic version of the treated unit using a weighted combination of untreated units. These weights are chosen to closely match the treated unit's outcome trajectory and covariates in the pre-treatment period.

This method was originally proposed by Abadie et al. [2010] to study the economic impact of California's 1988 tobacco control program. Rather than comparing California to a single state, SCM used a weighted average of other U.S. states to construct a "synthetic California" that closely mirrored its economic indicators before the intervention. Any divergence between the treated unit and its synthetic control after treatment can then be attributed to the intervention, under the assumption that the synthetic control approximates the counterfactual trajectory the treated unit would have followed in the absence of treatment.

Compared to standard DiD, SCM is more flexible and data-driven. It relaxes the requirement that the treatment and control units follow identical trends and instead ensures a close match in the pre-treatment period. This makes SCM particularly valuable in comparative case studies or when

few treatment units are available, though it also comes with limitations—such as sensitivity to model specification and the requirement for a rich pool of potential control units.

B Work History Italian Panel Data

In Italy, the organisation that collects social insurance contributions and distributes social security benefits, such as pensions, maternity leave, and unemployment benefits, is the Istituto Nazionale della Previdenza Sociale (INPS). As such, INPS gathers data on significant workforce segments, both active and inactive. The reference population comprises all individuals employed by private firms, workers with quasi-dependent employment arrangements, self-employed, retirement spells, and non-working spells in which the individual received social benefits, like unemployment subsidies or mobility benefits. The workers for whom activity is not observed are those who worked as freelancers and have an autonomous security fund. The observed group represents all manufacturing, construction, and services production sectors. However, it does not cover public employment, which involves approximately 3.5 million people, predominantly in the education and health sectors. Certain sectors, such as agriculture, are not fully represented in INPS data since its data does not cover any activity in the shadow economy. If an individual is observed working one year in a private company, and then he/she starts working in the shadow economy, INPS will register only that one year the individual was legally working.

The Work History Italian Panel (WHIP) [Leombruni et al., 2010, Bena et al., 2012] consists of a systematic sample of 1 in 15 individuals drawn from the INPS database based on their date of birth. This database allows us to track the employment histories of sampled individuals, including all periods of employment recorded by INPS, retirement, and any time spent receiving social security benefits, such as unemployment subsidies or maternity leave. The WHIP currently covers the period from 1985 to 2019.

For our analysis, we limit the sample to WHIP observations recorded from 1990 to 2015 for training. We started in 1990 as the information's reliability improved significantly from that date onward. Additionally, we apply the following selection criteria to further refine our sample:

1. Have information until the end of the observed period (2015)
2. Effective period observed greater than or equal to half of the worker's potential period. Thus, we include only individuals observed for at least half of their maximum possible participation period, where labour force participation is assumed to start at age 30 and is bounded by the 1990–2015 data window and an 85-year lifespan. For example, an individual born in 1975 turns 30 in 2005, we expect to observe him/her from 2005 to 2015. If we observe him only from 2013 to 2015 (3 years), the ratio between effective (3) and potential (10) is 0.3. Therefore, we exclude this individual from the sample.
3. No missing date of birth
4. At least five records
5. Age of entry in the panel higher than 15 and lower than 80. We exclude those individuals who are too young or too old.
6. Fraction of returns or investment income over the total number of records lower than 90%. We exclude people who are fully detached from the workforce.

B.1 Labour Records

The primary individual information in WHIP is yearly income. This is the most important information for INPS to compute contributions and monitor social security benefits. Many other variables are attached to each yearly income. For our study, we focus on 15 income-related variables.

Demographic information WHIP records include an individual's demographic/background information. These are (1) sex, (2) birth date, and (3) macro-area of birth. In our case, sex is a binary variable that encodes male or female. We retrieve only the birth year from the birth date to encode the age when a labour event occurs. The macro-area of birth specifies one of the 5 Italian groups of regions (North-East, North-West, Center, South, or Island). There is a sixth category for foreign-born people.

Initial Number of Individuals	4032674
Selection Criteria	% Drop
1.	13.24
2.	16.45
3.	0.16
4.	6.5
5.	4.91
6.	13.83
Final Number of Individuals	1652877

Table 2: Sample selection. Each row in the table corresponds to a selection criterion. The second column reports the percentage of individuals discarded, regardless of the other selection criteria

Workplace information Another set of variables pertains to features of the workplace. Notably, only for working individuals the following information is stored, e.g., residents receiving a pension, unemployment benefits or rents, do not have any of these specified, while for a self-employed person we observe only the workplace location.

(4) Economic activity/Sector denotes the services or goods that the company produces. WHIP encodes this information through the ATECO classification system¹. ATECO is the national version of the European nomenclature, Nace Rev. 2, Regulation (EC) No 1893/2006 of the European Parliament and of the Council of 20 December 2006². The ATECO has a hierarchical tree-like system, each additional digit provides a more detailed breakdown of the service, see the example in the following table. For our study, we use only the first four digits of the ATECO code to balance informativeness and sample size of each category.

ATECO CODE	Definition
G	Wholesale and retail trade
45	Repair of motor vehicles and motorcycles
45.1	Trade in motor vehicles
45.11	Trade in passenger cars and light motor vehicles

(5) Enterprise size is encoded in 5 ordinal categories: less than 10 employees, between 10 and 19, between 20 and 199, between 200 and 999, and more or equal to 1000. Finally, (6) Workplace location can be one of the 107 Italian provinces, plus an additional category for foreign locations.

Individual income information The last set of features provides details about the individual's income and its nature. (7) Labour force status is specific to WHIP, i.e. it does not follow any international classification system. It describes the type of income, i.e. in what context the income is associated with a person. Examples of these statuses include: "Employee", "Pensioner", "Self-employed", "Unemployed", encompassing work-related and other socioeconomic statuses. "Employee", "Self-Employed, or "Para-Subordinate" (e.g. sub-contractors, consultants, people with work contracts but not all the benefits) have one additional modifying information, the (8) Working title which indicates the qualification in the job and may fall into one of 11 categories: in training, Workman, Clerk, Junior Manager, Senior Manager, technical-administrative, Sportsman, Artist, Voucher, Collaborator, or Professional.

For "Employee" records only, we have four additional modifiers: (9) work intensity, (10) maternity leave intensity, (11) sick leave intensity, and whether the work is (12) part-time or full-time. The three intensities describe the average number of weeks in a month when an employee was working, on maternity leave, or sick. We derive the intensity by dividing the overall number of weeks spent in a given category (e.g. working) by the total number of months the employment relationship lasted in a given year. Therefore, each record can take a maximum value of around 4.3 (52 weeks divided by twelve), and a minimum value of 0. Notably, maternity leave is only recorded for female employees. Finally, we discretise the intensity into five categories based on the rounded value. If, for example, the intensity work is zero, we encode it as <WRKINT_S0>, if the intensity is less than 1, we encode it as <WRKINT_S1>, for intensities greater than 4, they are encoded into the category <WRKINT_S4+>.

¹<https://codiceateco.it/sezioni>

²<https://eur-lex.europa.eu/eli/reg/2006/1893/oj/eng>

The final attributes are the (13) month the event started, its (14) duration in months within a year, and (15) income during the event. The nature of income differs depending on the labour force status. For example, for "Employees", "Self-employed", "Para-Subordinate", and "Rentiers", it is the reported income from which the INPS calculates social security contributions. For "Unemployed" and "Pensioner", the income is the amount that INPS provides to the individual. The raw version of the income is a yearly value; we divide it by the duration in months of a given labour force status within a year and derive a monthly income. We further adjust it for inflation, deriving a real monthly income, and discretise this value into 100 quantiles.

General	Number of Individuals	1652877
	Average number of events	30.48
	Median Year	2005
	Median Age	42
Background	% Female	37.1
	% North-West	22.6
	% North-East	18.4
	% Center	15.9
	% South	22.4
	% Islands	9.73
	% Foreign born	11
	% Missing Area of Birth	0.0005
	Median Year of Birth	1966

Table 3: Descriptive Statistics of the Dataset

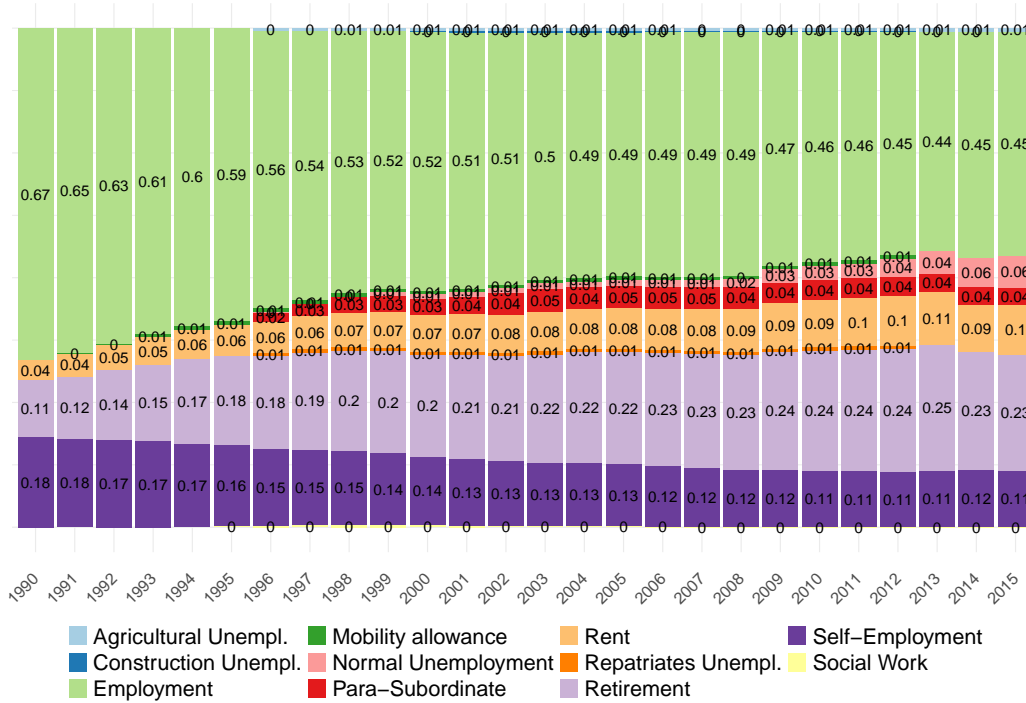


Figure 5: Labour Force Status composition for each year in the global dataset

Vocabulary The collection of all concept-tokens creates the vocabulary \mathcal{V} . The vocabulary is made up of tokens for all categories of each variable and has size $|\mathcal{V}| = 661$. The vocabulary \mathcal{V} is generated from the training subset and does not include all the possible categories in the data. Table 4 lists all variables and their possible categories.

Token Type	Variables	N. Categories	Encoding
Background Information	Year of Birth	86	1913-1998
	Sex	2	F-M
	Area of Birth	6	1-6 (Foreign)
Labour	Enterprise type	280	ATECO 4-digits
	Enterprise size	5	WHIP classification
	Work Location	110	Italian provinces codes
	Labour force status	11	WHIP classification
	Work title	11	WHIP classification
	Work Arrangements	2	Part time - Full time
	Work intensity	5	Threshold based
	Maternity leave intensity	5	Threshold based
	Sick leave intensity	5	Threshold based
	Income	100	Quantile based
	Start Month	12	1-12
Duration	12	1-12	
Special	Special	11	[PAD]...[UNK]

Table 4: Vocabulary specification

Labour life sequence Each life sequence is represented as a list of discrete tokens, encoding time-indexed events and their characteristics. Sequences are capped at a maximum of 1,560 tokens. Any sequence shorter is padded with a padding token, and any sequence longer is truncated starting from the earliest years (i.e. from the start of the sequence), ensuring that all input tensors are of consistent shape for training and inference. Longer sequences are truncated by whole years so as not to lose the temporal structure of the sequence (i.e. all tokens in a year are deleted until the sequence is at most 1,560 tokens long).

When an individual has no recorded activity in a given year, the year is still represented in the sequence. We then insert a silent event placeholder: <MONTH_1> followed by <DURATION_12> with no attributes in between, to preserve the temporal regularity of the sequence. The ordering of tokens within a sequence is chronological. Events that begin in the same calendar month are randomly shuffled relative to each other, regardless of their duration. This is based on the assumption that events co-occurring in the same month cannot be reliably ordered based on observed data, and shuffling them prevents the model from overfitting to arbitrary patterns in event ordering. Outside of these same-month shuffles, the rest of the sequence remains ordered. Besides same-month shuffling, we introduce a small amount of token dropout, randomly removing about 1% of tokens during training. This regularisation mechanism discourages the model from overfitting to missing data and promotes robustness. The dropout is uniformly applied and does not target any specific token type.

Inside each event, there is a meaningful and deliberate order to the tokens. Their order reflects a semantic priority derived from the downstream modelling goals. For example, income is placed before ATECO (economic activity), because for many of our tasks, we are more interested in how income can inform or predict the sector of employment, rather than the reverse. That is, we assume income to be more causally upstream in our use cases. While alternative orderings are possible, changing the token order within events would require retraining, as the model implicitly learns positional correlations. Nevertheless, this ordering can be adjusted in future work depending on the application.

The sequence lengths (measured as the number of tokens per individual life trajectory, excluding background information) have the following descriptive statistics

	Mean	Median	Mode	Minimum	Maximum
Tokens	232	220	128	21	1554

Table 5: Descriptive statistics of sequences

This example is not based on an individual in the dataset, any resemblance to a real individual is coincidental. Consider an example as an illustration of the encoding:

A3 | F | MONTH_1 | YEAR_1942,

i.e. a female born in January of 1942 in the Center region of Italy. Assume that in the first year of measurement (1990), she worked full time during the whole year, then had a year of no recorded activity, and then got another job in a different province for the entire following year:

[BOL] (0, 0) | MONTH_1 (1, 48) | [TIPO_1] (1, 48) | INCOME_20 (1, 48) | WRKT_1 (1, 48) | WRKP_XX (1, 48) | ATE_A123 (1, 48) | FSIZE_1 (1, 48) | FULL_TIME (1, 48) | WRKINT_S3 (1, 48) | SIKINT_S0 (1, 48) | MATINT_S0 (1, 48) | DUR_12 (1, 48) | [EOY] (1, 48) | MONTH_1 (2, 49) | DUR_12 (2, 49) | [EOY] (2, 49) | MONTH_1 (3, 50) | [TIPO_1] (3, 50) | INCOME_22 (3, 50) | WRKT_2 (3, 50) | WRKP_YY (3, 50) | ATE_A124 (3, 50) | FSIZE_1 (3, 50) | FULL_TIME (3, 50) | WRKINT_S3 (3, 50) | SIKINT_S0 (3, 50) | MATINT_S0 (3, 50) | DUR_12 (3, 50) | [EOY] (3, 50)

The numbers inside parentheses next to the tokens are the year (measured as years after 1989) and her age. Notice that the [EOY] token is measured with the current year and age, and once this token appears, the year and age increase by one. Hence, when the model generates an [EOY] token, time embeddings are updated deterministically. Each of her working spells is different because of its attributes, though for both of her working spells, she worked an average of 2 to 3 weeks each month and never took sick or maternity leave.

Her life sequence continues for every year until 2015, and when she is around 60 years of age, she retires and starts getting a pension from INPS:

[EOY] (12, 59) | MONTH_1 (13, 60) | [TIPO_1] (13, 60) | INCOME_39 (13, 60) | WRKT_2 (13, 60) | WRKP_YY (13, 60) | ATE_A124 (13, 60) | FSIZE_1 (13, 60) | FULL_TIME (13, 60) | WRKINT_S3 (13, 60) | SIKINT_S0 (13, 60) | MATINT_S0 (13, 60) | DUR_5 (13, 60) | MONTH_5 (13, 60) | [TIPO_10] (13, 60) | INCOME_35 (13, 60) | DUR_8 (13, 60) | [EOY] (13, 60) | MONTH_1 (14, 61) | [TIPO_10] (14, 61) | INCOME_35 (14, 61) | DUR_12 (14, 61) | [EOY] (14, 61)

Notice she still works for the first 5 months of 2005 and only starts receiving her pension in May. After that, she is likely to stay on a pension scheme until 2015.

C Model architecture

Transformers are a class of neural network architectures initially developed for natural language processing tasks, such as machine translation or text summarization [Vaswani et al., 2017], but are now being applied to a wide variety of sequence types from different domains, including protein discovery Consens et al. [2025], health predictions [Yang et al., 2023], music generation Agostinelli et al. [2023]. Their strength lies in the self-attention mechanism, which enables them to model long-range dependencies in sequential input.

One of the most influential *encoder-only* Transformer models is BERT (*Bidirectional Encoder Representations from Transformers*), introduced by Devlin et al. [2019]. BERT is trained using a masked language modelling (MLM) objective, where a subset of tokens in the input sequence is randomly masked, and the model learns to predict them using bidirectional context—i.e., both left and right tokens. This bidirectional attention mechanism enables BERT to build rich, context-aware representations of entire sequences, making it highly effective for discriminative tasks such as text classification, question answering, and semantic similarity. Since BERT processes the entire input at once, it excels at tasks that require a holistic understanding of the input sequence, rather than step-by-step prediction. An *encoder-only* version of our model is similar to Savcicens et al. [2024]’s Life2Vec, which is inspired by the BERT architecture and training objective.

In contrast, GPT (*Generative Pre-trained Transformer*) exemplifies a *decoder-only* architecture. Introduced by Radford et al. [2018], GPT is trained with an auto-regressive objective, predicting the next token in a sequence based solely on the preceding tokens. GPT uses causal (masked) self-attention, which restricts each token’s attention to preceding positions in the sequence, preventing

information from "leaking" from future tokens. Unlike BERT, GPT does not explicitly mask input tokens, but the causal attention mechanism ensures that generation proceeds in a left-to-right manner. This makes the GPT architecture particularly well-suited for generative tasks, such as language generation, sequential modelling, and, in our case, simulating counterfactual life sequences. Figure 6 illustrates the decoder-only architecture we train in this paper.

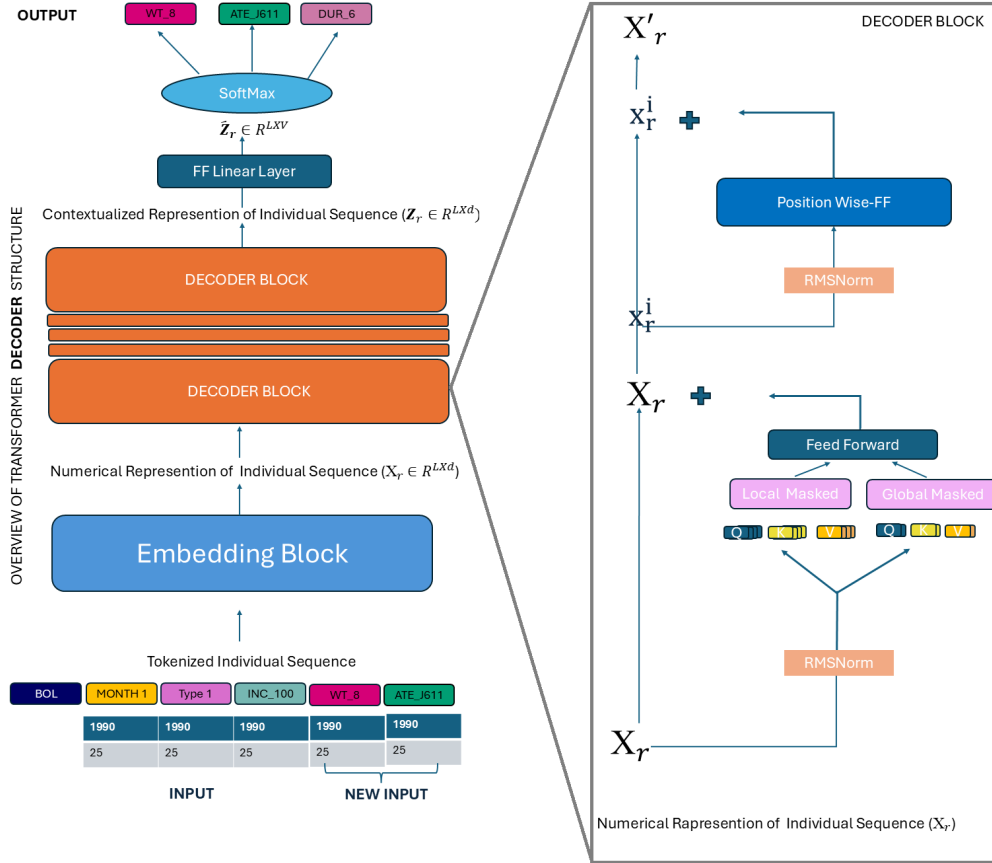


Figure 6: Overall architecture of the **decoder-only** model. Each tokenised life sequence is passed through an embedding block and a stack of decoder blocks. Each token—consisting of concept, age, and year information—is embedded using three components: concept embeddings retrieved from a learned lookup matrix \mathcal{E}_V (normalised by subtracting its mean), and temporal features (age and year) encoded via Time2Vec. These are combined with learnable positional embeddings to form the input token representations. The resulting sequence is processed through multiple decoder blocks, each structured to preserve the autoregressive nature of the task. Each block starts with RMS normalisation, followed by a masked multi-head attention layer (using the Performer mechanism with local and global heads), ensuring that each token only attends to preceding tokens. The output of the attention layer is combined with the input via a residual connection. This is followed by another RMS normalisation and a position-wise feed-forward layer, whose output is again added through a residual connection. Finally, the contextualised output representations are passed through a linear projection head and to a softmax function that assigns a probability to each token in the vocabulary. The predicted token is the one with the highest probability score.

Between the development of *encoder-only* models like BERT and *decoder-only* models like GPT, another approach combined the strengths of both: the *encoder-decoder* architecture. Popularised by models such as T5 (*Text-to-Text Transfer Transformer*), this architecture was initially inspired by earlier sequence-to-sequence models used in machine translation [Raffel et al., 2020]. In this setup, an encoder processes an input sequence—such as a question, a prompt, or a contextual situation—and produces a latent representation that is then consumed by a decoder to generate a corresponding output sequence, such as an answer, a summary, or a translated sentence. The decoder uses cross-attention

to condition its generation on the full encoded representation, effectively enabling the model to incorporate rich contextual information while generating responses in an autoregressive manner.

Encoder–decoder models are especially well-suited to tasks where there is a clear distinction between input and output roles, and where conditioning on the full input is crucial—examples include question answering, summarisation, and program synthesis. While this approach is more computationally demanding—requiring separate encoder and decoder stacks and more memory for cross-attention—it allows for greater flexibility and generality, especially in multi-modal or structured input scenarios. In our context of life sequence modelling, *encoder–decoder* architectures are particularly appealing when we wish to condition the prediction of future life trajectories on a fixed set of background covariates (e.g., age, sex, place of birth), which can be encoded once and used to guide generation through the decoder.

Figure 7 illustrates the encoder-decoder architecture we develop and train in this paper. The encoder (right side of the figure) processes a short, unordered sequence of concept tokens representing background characteristics (e.g., gender, education). Since these inputs are unordered, positional embeddings are omitted. Each token is passed through an embedding layer, then into a standard multi-head self-attention layer. RMS Normalisation is applied before both the attention and feedforward layers. The output of the attention layer is added back to the input via a residual connection. The final output is a fixed-length contextualised representation that conditions the decoder via cross-attention. The decoder (left side) follows an autoregressive design. Each concept token in a sequence (including age and year information) is passed through an embedding block that merges concept embeddings, age and year embeddings (via `time2vec`), and rotary positional encodings (RoPE) to capture temporal structure. The concept embeddings are drawn from a lookup matrix \mathcal{E}_V , with the sequence mean subtracted to stabilise learning.

The decoder comprises stacked blocks, each with three components: RMS Normalisation, a causal (masked) self-attention layer using Performer Attention, and a feedforward layer. In the first two decoder blocks, an additional cross-attention mechanism allows the decoder to attend to the encoder outputs. RMS Normalisation precedes attention and feedforward components, and residual connections are applied throughout. During training, the model is optimised for a next-token prediction objective, learning to generate plausible and coherent life sequences conditioned on prior events and background features.

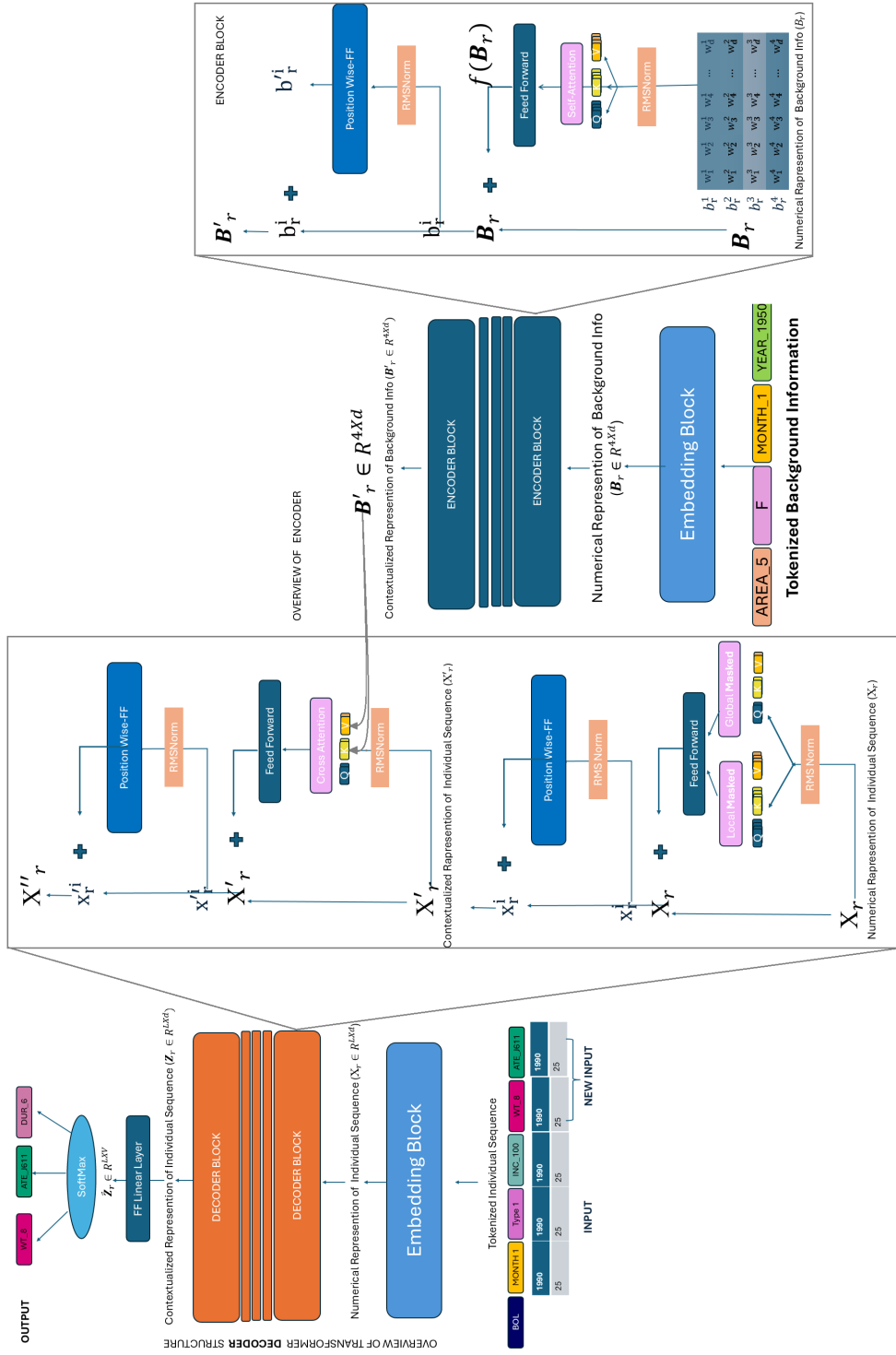


Figure 7: Overall architecture of the encoder-decoder model.

D Experimental details

Retirement Timing As a first causal benchmarking exercise, we evaluate the model’s ability to replicate the well-documented finding that month of birth influences retirement timing [Ardito et al., 2020]. Specifically, individuals born earlier in the calendar year tend to retire slightly later, due to institutional and lifecycle timing mechanisms.

To assess this, we select from the test set all male individuals born between 1940 and 1950, restricting the sample to those born in either January or December. To ensure a clean employment trajectory, we include only those who have been continuously and exclusively employed in standard employment, excluding individuals who were ever self-employed, para-subordinate, unemployed, or employed under special regimes (e.g., artists, athletes, or voucher-based contracts). We further restrict the sample to those whose first pension spell occurs between ages 55 and 68, and who exhibit no long gaps in their administrative records.

To reduce noise from incomplete information, we also exclude individuals with missing values in key attributes such as work province, economic sector (ATECO), income, and job title. After applying these criteria, the final evaluation set comprises 1,010 individuals.

For each of these individuals, we provide the model with their observed sequence up to the year before retirement, and task it with generating their life sequences forward until 2015. We therefore analyse whether the model both captures the correct retirement timing and the expected shift between those born in January and December.

Child Penalty The second exercise evaluates the model’s capacity to reproduce the income loss experienced by women following childbirth, a well-established finding in the causal literature on gender inequality in the labour market [Kleven et al., 2019, Casarico and Lattanzio, 2023].

From the test set, we selected a sample of women who had only held standard employment contracts throughout their recorded work histories. We identify mothers as those who experienced at least one maternity leave spell, defined by a maternity level intensity greater than one. To ensure sample homogeneity, we exclude individuals who were ever classified as managers or professional athletes, as these careers may follow atypical trajectories.

Further, we restrict the sample to women employed in southern Italian provinces at the time of childbirth, as here labour market dynamics tend to be more constrained [Carta et al., 2024]. To ensure high data quality, we retain only those individuals with less than 1% missing data across key variables: economic sector (ATECO), work province, income, and job title.

To allow for sufficient observation both before and after childbirth, we focus on women whose first childbirth occurs between the 5th and 20th year of their observed life course. This ensures a meaningful pre-treatment period for conditioning and a post-treatment period for simulation.

The final sample comprises 631 mothers. For each, we provide the model with their complete life sequence up to the year of childbirth, and generate the trajectory from that point until the end of the observation window. This allows us to evaluate whether the model captures the expected post-maternity income trend.

Mobility allowance duration The third exercise examines whether the model can replicate age-based differences in the duration of unemployment benefits, specifically the mobility allowance, a now-discontinued income support program for workers displaced by firm closures in Italy. As shown in Figure 5 less than 1% of records in our global sample fall under this category.

Under the policy rules in place until January 2017, the maximum benefit duration hinged on the worker’s age at the time of job loss. Workers over 40 were eligible for up to 24 months of benefits, while those under 40 could receive income support for 12 months [Brunello and Miniaci, 1997]. This sharp policy threshold makes it an ideal setting to test whether the model internalises and reflects such causal discontinuities in allowance’s duration.

We drew individuals with at least one registered episode of mobility allowance from the test set, who also have only standard employment or retirement spells in their histories. To increase homogeneity, we exclude individuals with any history of self-employment, artistic or athletic careers, or voucher-

based contracts. Additionally, we retain only those employed in northern Italian provinces at the time of firm closure; a worker from the south is allowed one additional year of benefits.

We restrict the sample to workers who began receiving the benefit between the ages of 30 and 50, and who have less than 1% missing data on key variables: economic sector (ATECO), work province, income, and job title. The resulting sample consists of 1502 individuals.

We provide the model with each individual’s life trajectory up to the year we first observe the unemployment episode. The model then generates the sequence from that point onward. This setup allows us to test whether the simulated unemployment duration reflects the correct age-based discontinuity in benefit length.

Out-of-sample Generation We randomly selected 1,500 individuals from the test set, specifically drawn from those used in the three causal inference benchmarking exercises. For each individual, we generated their life trajectory for 20 years beyond the last year observed in the training data (2015).

The purpose of this experiment is to evaluate the structural coherence of out-of-sample generations over an extended horizon. For each generated sequence, we identify the first year in which the model produces a structural inconsistency. Consistency means that each calendar year must begin/end with an End-of-Year <EOY> token, followed by a valid combination of monthly tokens and corresponding durations. These can be empty, i.e. no event, or include a valid life event, but must respect the order: month, then optional content, then duration. Inside each year, there must be at least one event, even if empty (so no repeated <EOY> tokens). A duration token must be followed either by another month token or an <EOY> token indicating the start of the next year, and <EOY> tokens must always be followed by a month token.

Once a structural failure is detected in a given sequence, we record the year of failure and disregard any subsequent tokens, even if the sequence appears to recover. We then plot the density of the failure years to analyse how long the model maintains structural validity over time.

E Additional results

	Accuracy	Precision	Recall	F1 Score	Perplexity
0 known years	0.6225	0.6868	0.6225	0.6427	0.7288
1 known year	0.6773	0.7216	0.6773	0.6895	0.6937
5 known years	0.6883	0.7285	0.6883	0.6991	0.6727
10 known years	0.7039	0.7409	0.7039	0.713	0.6466

Table 6: **Decoder-only** test set metrics for next-token prediction, macro-averaged across the vocabulary, conditioning on 0, 5, 1 and 10 initial years of sequence.

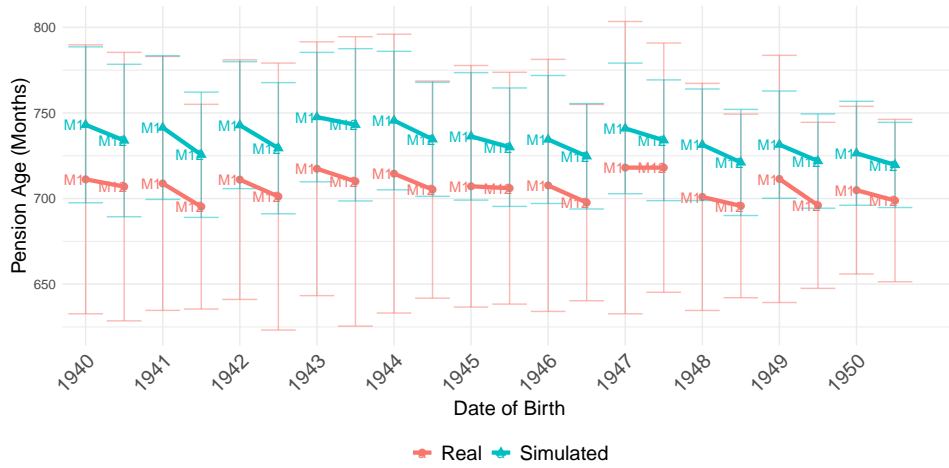


Figure 8: Real and **decoder-only** model-generated (blue) average pension ages—measured in months—for male individuals born between 1940 and 1950, stratified by birth month (January = M1, December = M12). Each point indicates the cohort-specific average retirement age for individuals born in January or December, with vertical bars representing a one standard deviation range.

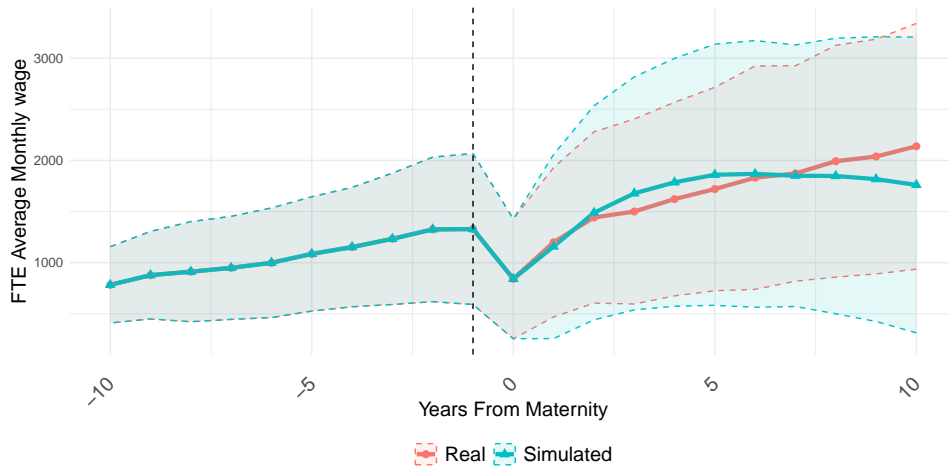


Figure 9: Real and **encoder-decoder** model-generated trajectories of average monthly income for working mothers in a 10-year window before and after their first maternity leave episode (Years From Maternity = 0). The solid lines represent the average monthly income, while the shaded areas denote the one standard deviation range.

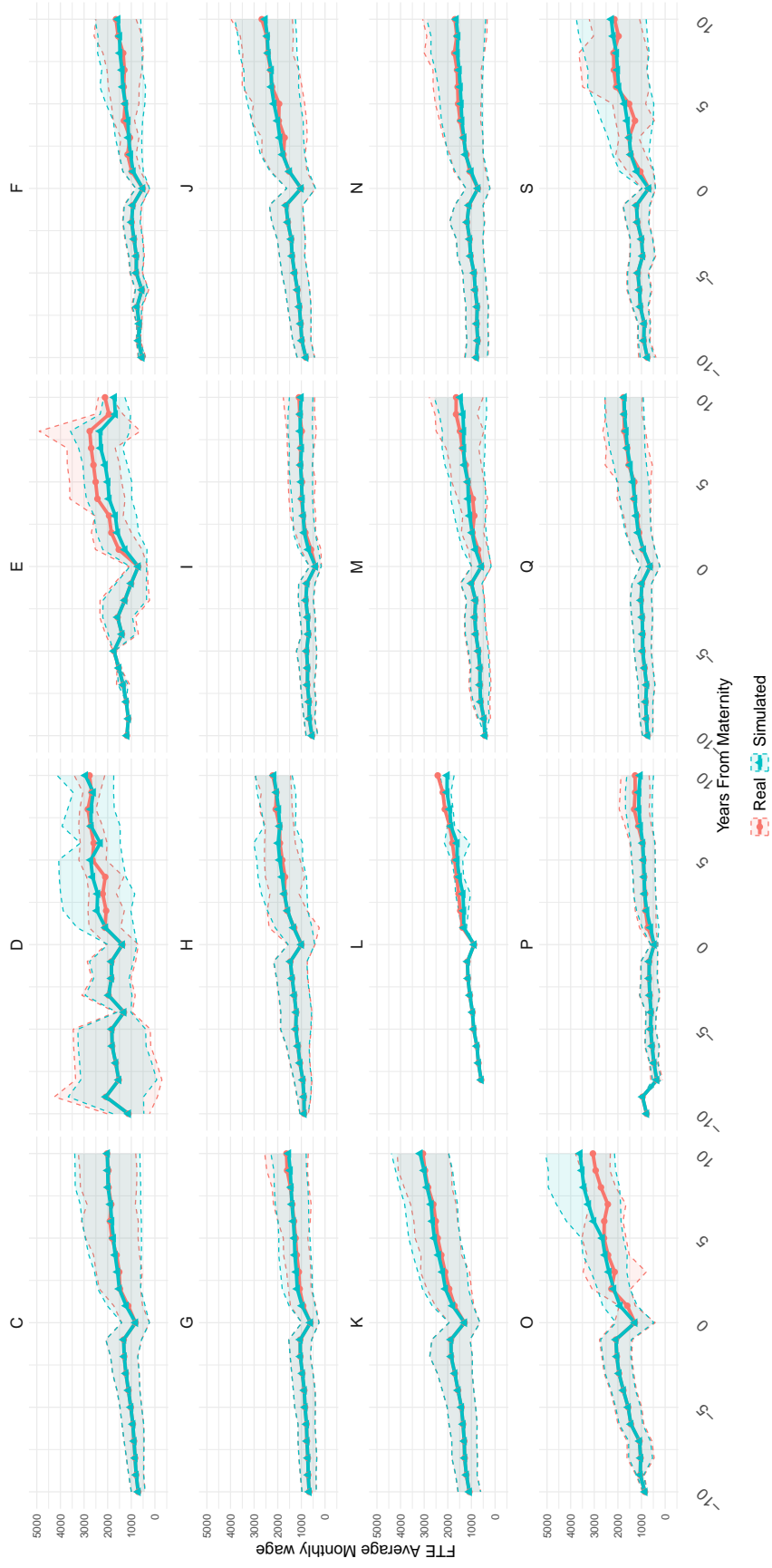


Figure 10: ATECO grouped real and **decoder-only** model-generated trajectories of average monthly income for working mothers in a 10-year window before and after their first maternity leave episode (Years From Maternity = 0). The solid lines represent the average monthly income, while the shaded areas denote the one standard deviation range.

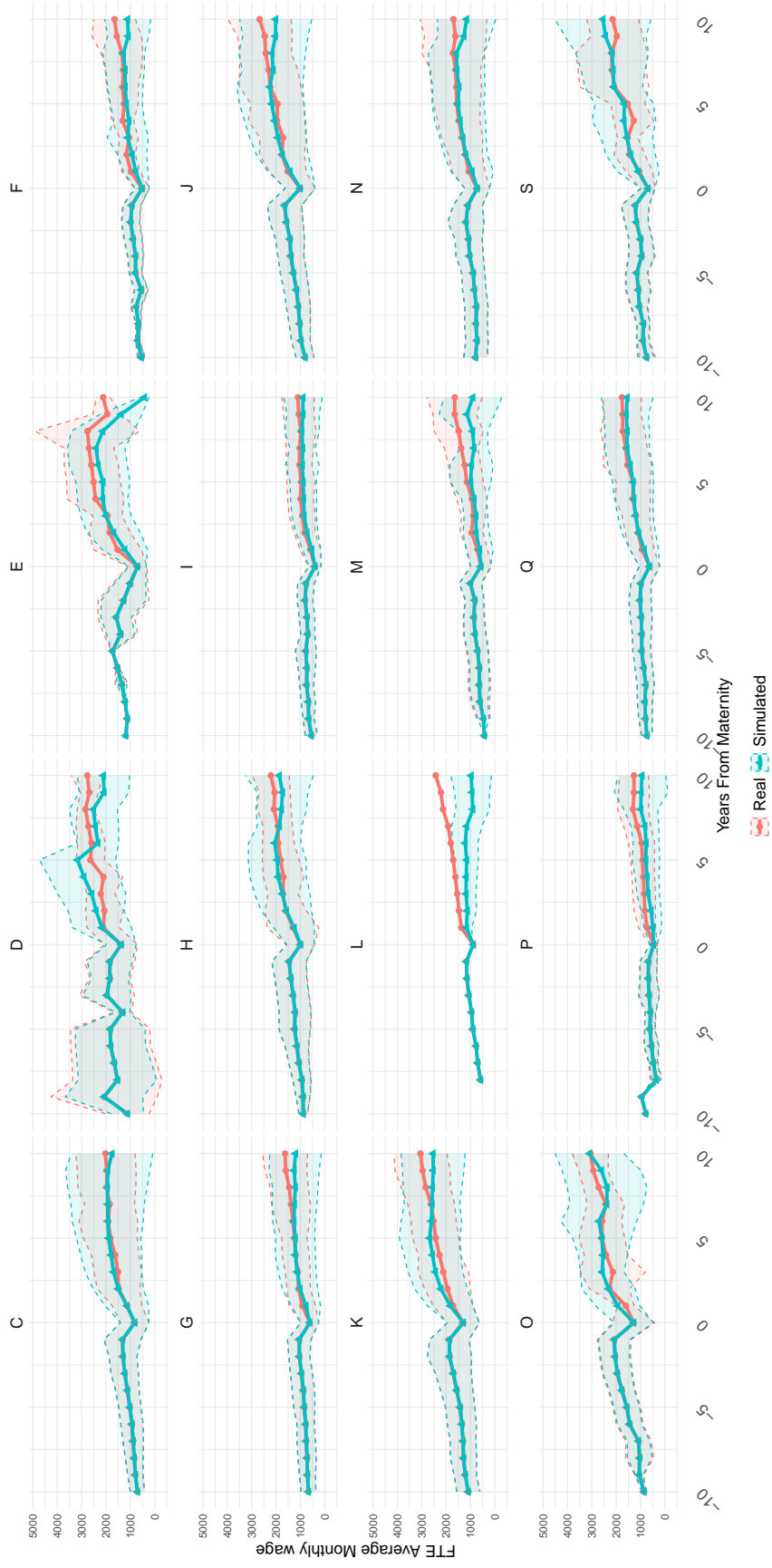


Figure 11: ATECO grouped real and **encoder-decoder** model-generated trajectories of average monthly income for working mothers in a 10-year window before and after their first maternity leave episode (Years From Maternity = 0). The solid lines represent the average monthly income, while the shaded areas denote the one standard deviation range.

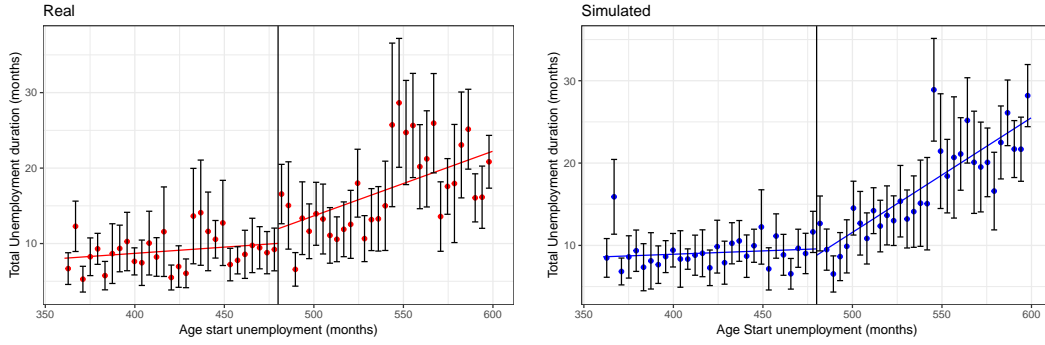


Figure 12: Real and **decoder-only** model simulated average duration with 90% confidence interval of mobility allowance receipt duration as a function of worker age at job loss in months in a 10-year bandwidth around the 40 years old threshold

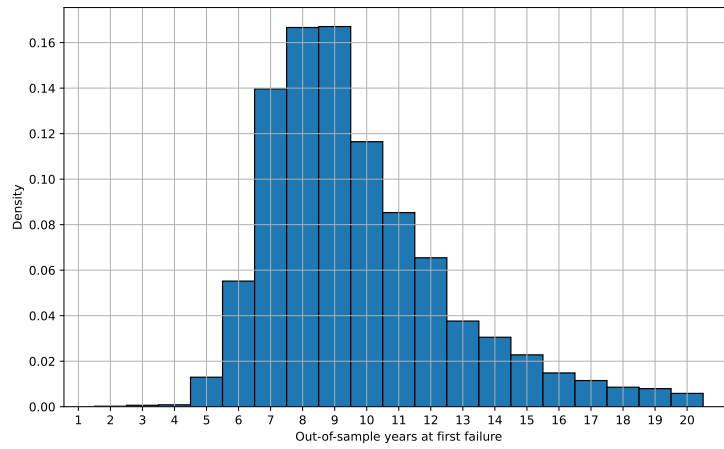


Figure 13: Density plot for the **decoder-only** out-of-sample year when the model generates incorrect sequences, 5% of the observations were able to complete the 20 years of generation without failures.

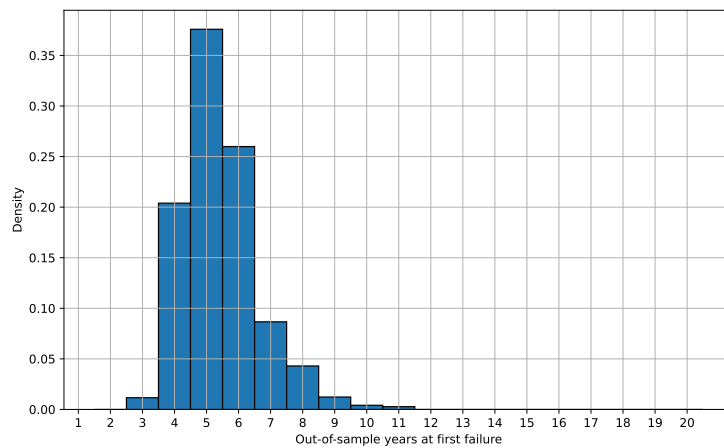


Figure 14: Density plot for the **encoder-decoder** out-of-sample year when the model generates incorrect sequences, 0% of the observations were able to complete the 20 years of generation without failures.

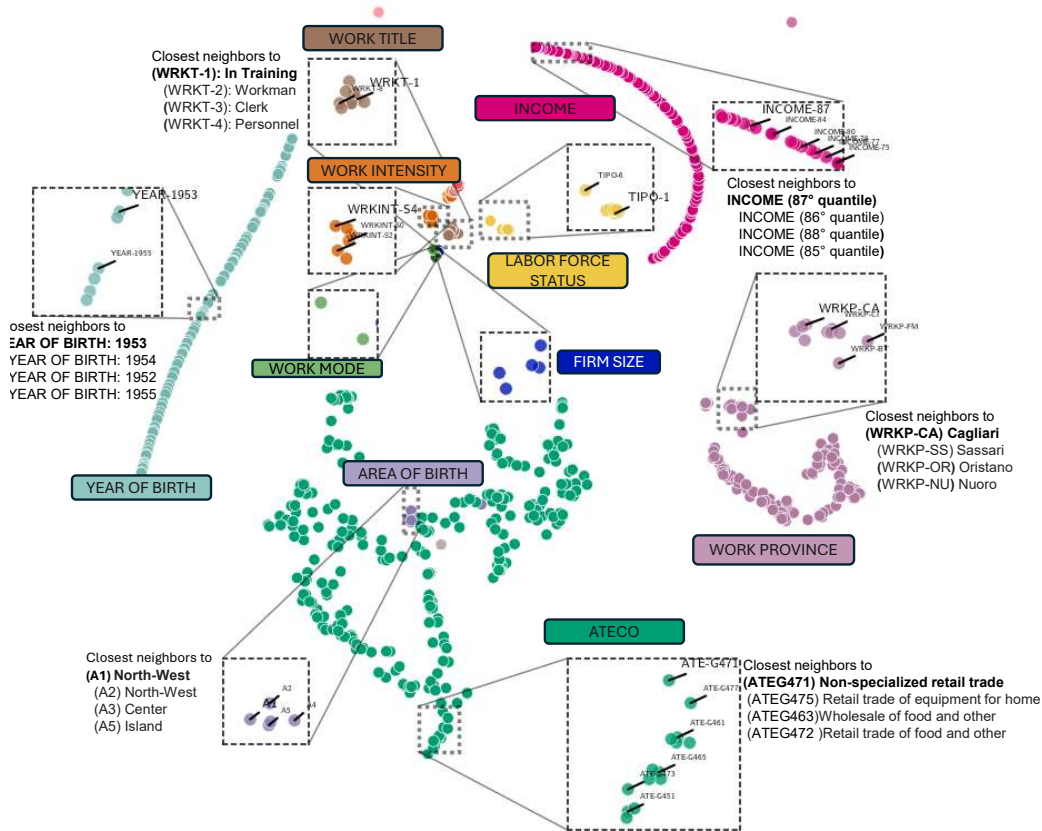


Figure 15: Two-dimensional projection of the learned embedding space from the **encoder-decoder** model, visualized using the PaCMAP dimensionality reduction technique [Wang et al., 2021]. Each point represents a token from the vocabulary ($|\mathcal{V}| = 661$), with different colours denoting different token categories. Several regions of interest are highlighted with zoomed-in views, each showing the top three nearest neighbours of a specific token. Neighbour relationships are computed using cosine distance in the original high-dimensional embedding space ($d = 240$).

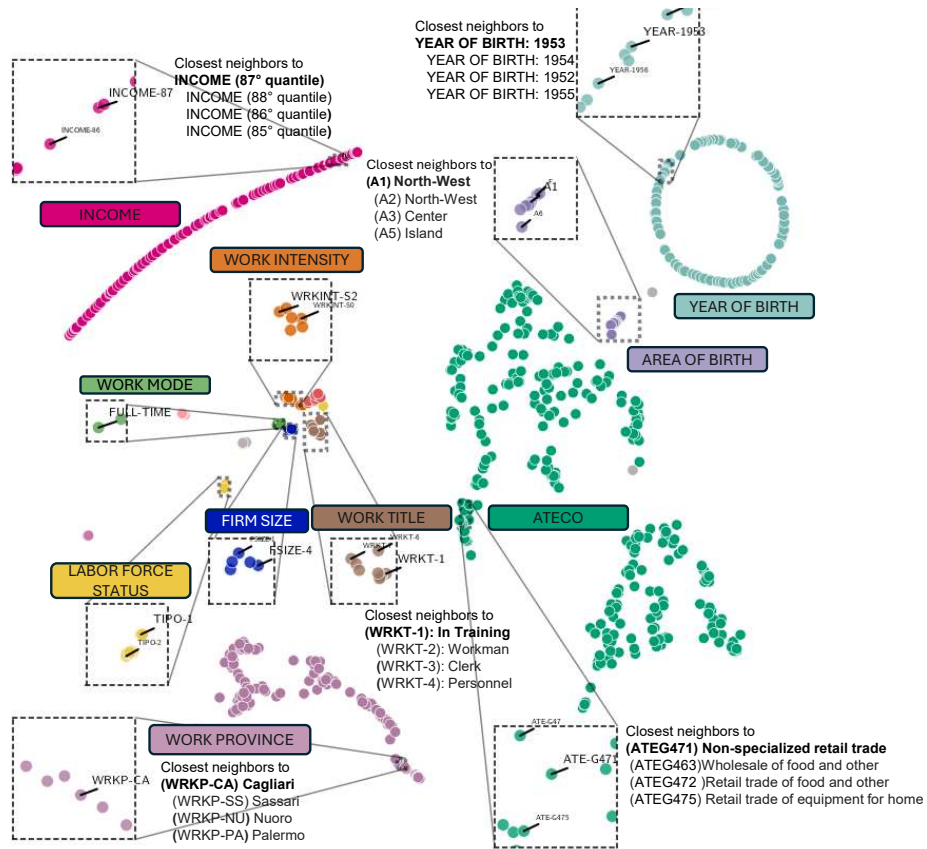


Figure 16: Two-dimensional projection of the learned embedding space from the **decoder-only** model, visualized using the PaCMAP dimensionality reduction technique [Wang et al., 2021]. Each point represents a token from the vocabulary ($|\mathcal{V}| = 661$), with different colours denoting different token categories. Several regions of interest are highlighted with zoomed-in views, each showing the top three nearest neighbours of a specific token. Neighbour relationships are computed using cosine distance in the original high-dimensional embedding space ($d = 240$).